2015 14th International Conference on Computer-Aided Design and Computer Graphics

Novel, Robust, and Efficient Guidewire Modeling for PCI Surgery Simulator based on Heterogeneous and Integrated Chain-Mails

Weiwei Wang
Beihang University

Shuai Li*
State Key Laboratory of Virtual Reality Technology and Systems, Beihang University, lishuai@buaa.edu.cn

Hong Qin
Stony Brook University

Aimin Hao
Beihang University

***Abstract*—Despite the long R&D history of interactive minimally-invasive surgery and therapy simulations, the guidewire/catheter behavior modeling remains challenging in Percutaneous Coronary Intervention (PCI) surgery simulators. This is primarily due to the heterogeneous heart physiological structures and complex intravascular inter-dynamic procedures. To ameliorate, this paper advocates a novel, robust, and efficient guidewire/catheter modeling method based on heterogeneous and integrated chain-mails, that can afford medical practitioners and trainees the unique opportunity to experience the entire guidewire-dominant PCI procedures in virtual environments as our model aims to mimic what occurs in clinical settings. Our approach's originality is primarily founded upon this new method's unconditional stability, real-time performance, flexibility, and high-fidelity realism for guidewire/catheter simulation. Considering the front end of the guidewire has different stiffness with its conjunctive slender body and the guidewire length is adaptive to the surrounding environment, we propose to model the spatially-varying six-degree of freedom behaviors by solely resorting to the generalized 3D chain-mails. Meanwhile, to effectively accommodate the motion constraints caused by the beating vessels and flowing blood, we integrate heterogeneous volumetric chain-mails to streamline guidewire modeling and its interaction with surrounding substances. By dynamically coupling guidewire chain-mails with the surrounding media via virtual links, we are capable of efficiently simulating the collision-involved inter-dynamic behaviors of the guidewire. Finally, we showcase a PCI prototype simulator equipped with haptic feedback for mimicing the guidewire intervention therapy, including pushing, pulling, and twisting operations, where the built-in high-fidelity, real-time efficiency, and stableness show great promise for its practical applications in clinical training and surgery rehearsal fields.**

***Keywords*-guidewire simulation; heterogeneous chain-mails; guidewire-vessel interaction; guidewire-blood interaction; PCI simulator; haptic feedback;**

I. Introduction

Although many methods, ranging from simple spring-mass structure [1], moderately complex kirchhoff elastic rod [2] to complex Cosserat-theory-based models [3], have been employed to simulate the guidewire behaviors, suffering from the heterogeneous heart physiological structures and complex intravascular inter-dynamic procedures, the guidewire/catheter behavior modeling is still challenging in PCI surgery simulation due to lacking magic tradeoffs among seemingly competing criteria of unconditional stability, real-time performance, adequate flexibility, and high-fidelity realism. In particular, key technical challenges are highlighted as follows.

First, since heart has tortuous 3D blood flow pathways with multiple inlets and outlets, PCI simulation involves complex guidewire-dominant procedures, which requires the simulated guidewire should have six degrees of freedom. And [4] states that real-time efficiency is more important than accurate physical simulation in response to simulated interventions, to improve efficiency while retaining certain simulation accuracy simultaneously, it is nontrivial to design a robust and efficient geometric/physical model to depict and control the guidewire's behaviors with high fidelity.

Second, to facilitate the feeding direction tuning, the guidewire usually has a small segment of relatively-soft hook in the front end, whose stiffness is different from its connecting guidewire body. In addition, the discrete sampling of the guidewire should be adaptive to the surrounding environment. This makes the desired spatially-varying guidewire behavior model even more unimaginable.

Third, the heart is a four-chambered muscular organ containing an involuntary conduction system, which pumps blood throughout the blood vessels by repeated, rhythmic contractions. It is hard to simulate the dynamic coupling among guidewire, blood, and blood vessels. Thus, even if fully physics-based models can mimic such complex mechanics, the inevitable computation burden can not satisfy the interactive requirement of PCI surgery operations. Meanwhile, the stability is also a nontrivial problem that is commonly occurred in fully physics-based systems.

To tackle the aforementioned challenges, we focus on a brand-new, integrated, and robust guidewire modeling method towards its high-performance simulation and interactive response to the beating vessels and flowing blood in the PCI surgery simulator. Our approach is a generalized 3D chain-mail model with heterogeneous dynamics, enabling tight coupling of guidewire and its surrounding media in a unified solution. This is the first research attempt in adapting 3D chain-mail models to PCI simulation in VR. Fig. 1 intuitively illustrates the architecture of our method. Specifically, the salient contributions can be summarized as

978-1-4673-8020-1/15 $31.00 © 2015 IEEE
DOI 10.1109/CADGRAPHICS.2015.22

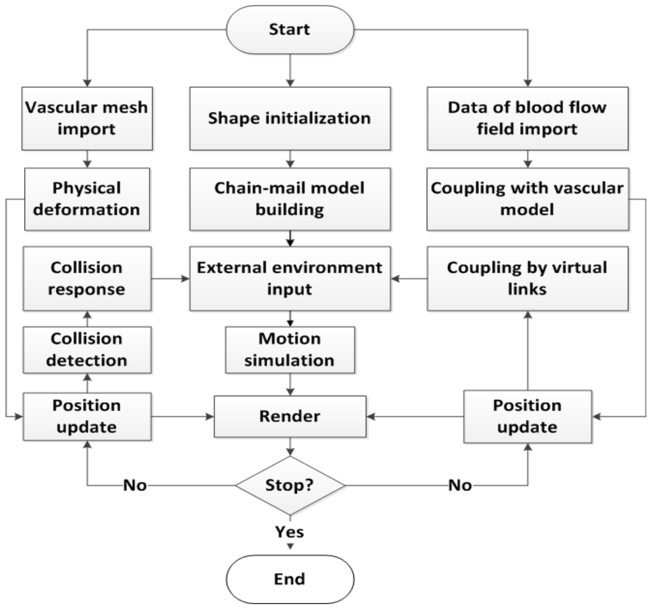

Figure 1. The flowchart of our new guidewire simulation method.

follows:

- We propose a spatially-varying six-DOFs (degrees of freedom) guidewire behavior model based on the generalized 3D chain-mails, which allows to handle the soft guidewire tip and its more rigid body in a simple and consistent way, and at the same time, can accommodate the overall guidewire length and its discrete representation to be adaptively modified according to the specific PCI intervention and the surrounding intravascular environment.
- We synchronously incorporate the surrounding-media interactions into the 3D chain-mails based guidewire model by streamlining the representation of vessel and blood with heterogeneous volumetric chain-mails and coupling their motion constraints based on the dynamically constructed virtual chain-mail links, which enables stable and real-time integrated behavior simulation among guidewire, blood flow, and vessel wall.
- We augment our guidewire simulation by integrating it with a PCI-specific force feedback device, together with penalty force based haptic feedback calculation, FEM-based tissue deformation, ray-casting based X-ray simulation, and 3D realistic rendering, which collectively give rise to the concerted efforts towards physical, visual, haptic, and procedural realism of PCI simulator, and also contribute to many other VR-based interactive simulations.

II. Related Work

Physics-based Guidewire Modeling and Simulation. Mass-spring model is intuitive and easy to understand [5], [6], however, it is hard to handle material torsion [7], while a guidewire being inserted into the blood vessel must undergo rotation. Mi et al. [8] proposed a multi-body mass-spring model by discretizing the guidwire into tip, link, and body. As for more complex physical models, FEM-based method is also very popular in guidewire simulation. Wei et al. [9] used 3D FEM-based beam element to simulate the guidewire, where each beam consists of two six-DOF nodes (three degrees for translation and the other three for rotation). The FEM-based method is more physically realistic, but suffers from being computationally expensive [10]. Besides, the Cosserat-based approaches consider the material frames when formulating the strain-stress relations of guidewire. For example, Tang et al. [11] proposed a real-time and realistic elastic rod model to simulate minimally invasive vascular interventions by limiting the guidewire to move along the centerline of the vessel. Sueda et al. [12] proposed a general framework to handle the large-scale deformation of highly constrained strands but without torsion. Recently, Mao et al. [3] designed a Cosserat-based guidewire model, which affords the guidwire to freely move (forward or backward), bend, or twist subject to collision contact, however, they ignored the guidewire-blood interaction. Although Cosserat-based method can obtain high physical accuracy, it is not stable, and needs to consume large amount of time to handle the continuous interaction with the surrounding environment.

Non-physics-based Guidewire Modeling and Simulation. Kaldoret et al. [13] addressed the simulation of knitted cloth at the yarn level, wherein the yarn is simulated with a single spline curve. Theetten et al. [14] proposed a spline based model to handle the physical simulation of deformable curve-shaped objects. Although these models can achieve good performance, they are hard to handle material torsion. Ganji et al. [15] employed the forward kinematics approach to predict the catheter's tip position by assuming the catheter bends with zero torsion and constant curvature. Rungjiratananon et al. [16] simulated complex hairstyle by employing an overlapped chain-shape-matching method and neglecting the torsion deformation. Non-physical models have advantages in efficiency and stableness for the guidewire simulation in complex environment, but they can only achieve physically-plausible effects.

Inter-Dynamic Behavior Coupling. Considering the influence on guidewire behaviors from flowing blood, we mainly review the coupling between the blood flow field and guidewire, which belongs to solid-fluid coupling issue. Akinci et al. [17] proposed a novel, versatile method for the two-way coupling of SPH fluids and rigid bodies by using boundary particles to sample the surface of rigid objects. Another two-way coupling technique is proposed to manipulate the forces between fluids and hair by Lin [18], wherein the motion of hair and fluids is simulated by evaluating the hydrodynamic forces with SPH-based boundary handling techniques. How to effectively handle collision for long

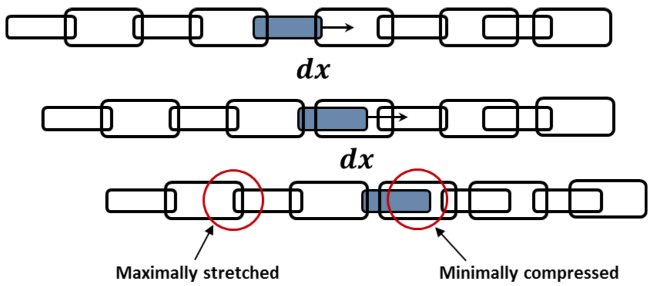

Figure 2. The fundamental principle of the basic chain-mail model. The black arrow means the moving vector of the ”sponsoring” element, represented by the blue-filled rectangle. When the distance of adjacent neighbors is less than the minimal compression or larger than the maximal stretch, elements adjust to satisfy the constraint, indicated with the red circle.

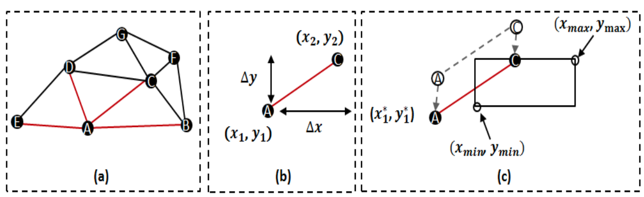

Figure 3. Illustration of the chain-mail updating rule. (a) An arbitrary chain-mail arrangement. (b) The initial state of the ”sponsoring” element A and the ”affected” neighbor element C. (c) When A moves, C should move to the nearest point within the valid region.

curve-shaped deformable models is also nontrivial. Servin et al. [19] described an approach for interactive simulation of wires contacting with rigid bodies using massless contact nodes. But their model can not handle self-contacts in high-tension regions. Durville [20] proposed a contact-friction model to simulate knot tightening, which can detect various contact configurations between elastic beams.

III. Guidewire Modeling based on 3D Chain-Mails

A. Overview on Generalized Chain-Mail Model

3D Chain-mail model is designed to deform large data sets at interactive rates, which permit to directly manipulate the original data while giving rise to efficient and stable deformation calculation [21]. When manipulating the volumetric object, each of its local elment will be stretched or compressed or rotated according to the allowable distance and shearing constraints between neighboring elements. The movement of each element depends only on the positions of its nearest neighbors. Fig. 2 illustrates the fundamental principle of the basic chain-mail model.

Li et al. [22] proposed an extension to the original chain-mail algorithm allowing non-uniform rectilinear meshes to be modeled. In the generalized chain-mail model, each element can be arbitrary positioned, and is linked to any number of neighbors; and it can be extended to any dimension. As shown in Fig. 3(a), we illustrate the generalized chain-mail model in 2D. Element A has four neighbors: B, C, D, and E. When A moves to a new position, its neighbors update their positions according to certain updating rules. Fig. 3(b) shows the initial positions of A and C, Fig. 3(c) shows the potential valid region of C, controlled by the compressing (through minDx), stretching (through maxDx) and shearing (through maxShearDy) constraints. If C is in the valid region, we do not need to move it, and we can continue to process the next neighbor. If C lies outside the valid region, we move it to the nearest position within the region, and the other neighbors in the lists are processed in turn.

B. Discrete Representation of Guidewire

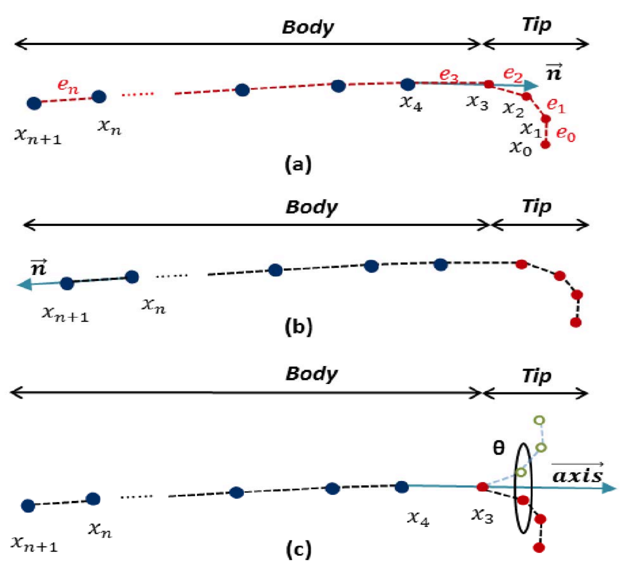

Figure 4. Illustration of different chain-mail constraints corresponding to the pushing, pulling, and rotating operations. In (a) and (b), the blue arrow means the direction of the translation. In (c), the blue arrow is the rotation axis and θ means the rotation angle.

Medical guidewire can be treated as elastic object that tends to bend or twist rather than stretch. By manipulating the end of the guidewire, the body should immediately propagate the translation or rotation to the tip. A high-fidelity simulation should reflect the subtle dynamics of the guidewire tip when the guidewire is being steered around a bifurcation.

We construct the guidewire representation model based on the generalized 3D chain-mails. We discretize the guidewire as a chain of small segments, and each segment denotes a small rigid rod, which is neither compressible nor bendable. And the hinge point connecting two segments controls the allowable local bending. As shown in the Fig. 4. By specifying spatially-varying control parameters for the body and tip, our chain-mail model can represent heterogeneous guidewire behaviors.

Pushing. As shown in Fig. 4(a), when the guidewire is pushed, the translation direction of the first chain-mail in the guidewire body is calculated by normalizing vector v, which is obtained by subtracting the position of the first tip chain-mail from that of the last tip chain-mail, respectively denoted as $x0$ and $x3$. Then the first body chain-mail will translate along the direction v according to the speed control parameter t. Taking the first body chain-mail as the sponsoring element, the translation is then sequentially propagated to other chain-mails under the compressing and stretching constraints (and shearing constraints).

Pulling. As shown in Fig. 4(b), when the guidewire is pulled, the last body chain-mail is moved along the normalized body direction v, which is calculated by subtracting the position of the last two chain-mails of the guidewire body. Analogously, taking the last body chain-mail as the sponsoring element, the positions of other chain-mails can be updated under the compressing and stretching constraints (and shearing constraints).

Rotation. As shown in Fig. 4(c), when the guidewire is rotated, we can get the rotation axis by normalizing the vector obtained from the first two chain-mails of the guidewire body. And then the first tip chain-mail will be rotated with an angel θ, which will further lead other chain-mails to move under the shearing constraints (and compressing and stretching constraints).

C. Numerical Computation of Guidewire Dynamics

Based on the constructed chain-mail model, we can conduct the guidewire deformation via two steps. In the geometric deformation step, when arbitrary chain-mail moves, the motion is sequently transmitted to its neighboring chain-mails guided by the spatially-varying compressing, stretching, and shearing constraints. In the physical optimization step, each chain-mail's position will be locally adjusted to keep the previous shape as rigid as possible, so that the system can arrive at the minimum energy state as quickly as possible.

Geometric Deformation. In our guidewire model, each chain-mail has two neighbors except the two terminal ones. Supposing the chain-mail $P(x_1, y_1, z_1)$ is the sponsoring element, and the chain-mail $Q(x_2, y_2, z_2)$ is one neighbor of P, then we have:

$$\begin{cases} \Delta x = |x_1 - x_2| \\ \Delta y = |y_1 - y_2| \\ \Delta z = |z_1 - z_2| \end{cases} . \tag{1}$$

When P moves to the new position $P^*(x_1^*, y_1^*)$, we can calculate the potential valid region of Q as:

$$\begin{array}{l} Q^* = \{(x, y, z) : x_{min} \leq x \leq x_{max}, \\ y_{min} \leq y \leq y_{max}, \\ z_{min} \leq z \leq z_{min}\} \end{array} . \tag{2}$$

If $x_2 \geq x_1, y_2 \geq y_1$ *and* $z_2 \geq z_1$, we can get

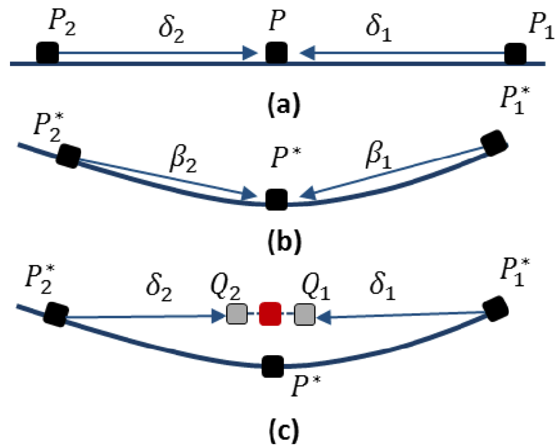

Figure 5. Illustration of physical optimization. From top to bottom: initial shape, deformed shape, optimized shape of the three guidewire chain-mails.

$$\begin{cases} x_{min} = x_1^* + (\alpha_{min}\Delta x - \beta(\Delta y + \Delta z)) \\ x_{max} = x_1^* + (\alpha_{max}\Delta x + \beta(\Delta y + \Delta z)) \\ y_{min} = y_1^* + (\alpha_{min}\Delta y - \beta(\Delta z + \Delta x)) \\ y_{max} = y_1^* + (\alpha_{max}\Delta y + \beta(\Delta z + \Delta x)) \\ z_{min} = z_1^* + (\alpha_{min}\Delta z - \beta(\Delta x + \Delta y)) \\ z_{max} = z_1^* + (\alpha_{max}\Delta z + \beta(\Delta x + \Delta y)) \end{cases} . \tag{3}$$

If $x_2 < x_1$, then the definitions of x_{min} and x_{max} change to

$$\begin{array}{l} x_{min} = x_1^* - (\alpha_{max}\Delta x + \beta(\Delta y + \Delta z)) \\ x_{max} = x_1^* - (\alpha_{min}\Delta x - \beta(\Delta y + \Delta z)) \end{array} . \tag{4}$$

Similar cases will occur when $y_1 < y_2$ or $z_1 < z_2$. And different settings for the parameters $\alpha_{min}, \alpha_{max}$ *and* β make the guidewire heterogeneous in slender body and soft tip.

Physical Optimization. As shown in Fig. 5, we further refine the chain-mail positions by minimizing the deformation energy of the entire guidewire. Given the initial position of chain-mail $P(x, y, z)$ and its two neighbors $P_1(x_1, x_1, x_1), P_2(x_2, x_2, x_2)$, we can obtain their relative-position vectors δ_i as

$$\delta_1 = P - P_1; \delta_2 = P - P_2. \tag{5}$$

After deformation, P moves to the new position, we can calculate its displacement vector β_i as:

$$\beta_1 = P^* - P_1^*; \beta_2 = P^* - P_2^*. \tag{6}$$

Therefore, according to the Hooke's Law, we can formulate the deformation energy as:

$$E = \textstyle\sum_{i=1}^{2} \|\beta_i - \delta_i\|_2^2. \tag{7}$$

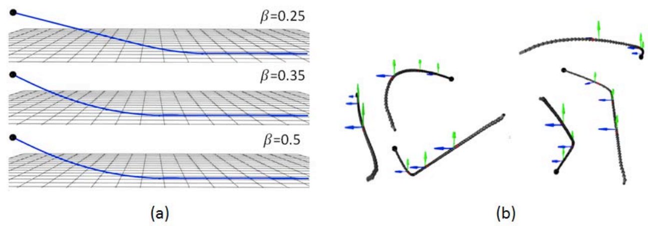

Figure 6. Heterogeneous guidewire simulation results. (a) From top to bottom,the shearing parameters are respectively set to 0.25, 0.35, 0.5, with the same compressing and stretching parameters. (b) The guidewire deformation results obtained by manipulating its soft tip with pulling, pushing, and twisting operations.

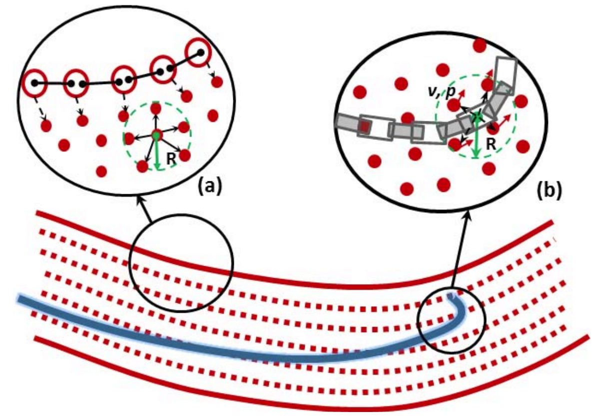

Figure 7. Illustration of heterogeneous chain-mails based coupling model. (a) vessel-blood coupling model. Red circles connected by black lines represent the vascular chain-mail model. Red points connected by green arrows represent the blood-field chain-mail model. The black-dotted lines are the virtual vessel-blood links. (b) guidewire-blood coupling model. Conjoint rectangles represent the guidewire chain-mails. Black-dotted lines are the virtual guidewire-blood links.

Then we need to calculate the new position of P^* to minimize the energy. By defining:

$$Q_1 = P_1^* + \delta_1; Q_2 = P_2^* + \delta_2; \tag{8}$$

we can rewrite the energy formula with Q_i as

$$E = \sum_{i=1}^{2} \|P^* - Q_i\|_2^2. \tag{9}$$

Minimize the energy, we can get the optimized position of P^* as the centroid of the Q_1Q_2.

$$P^* = \frac{Q_1+Q_2}{2}. \tag{10}$$

As described above, different materials can be simulated by adjusting the compressing, stretching, and shearing parameters respectively: α_{min}, α_{max} and β. In Fig. 6(a), one end of the guidewire is fixed to the wall, because of the gravity, the guidewire falls and collides with the ground spontaneously. Different shearing parameters lead to different deformation degrees. It shows that the larger the shearing parameter is, the greater the bending degree will be, which means the object is softer. Correspondingly, being similar to elastic ropes, a large proportion of the guidewire contacts with the ground. On the contrary, the small shearing parameter gives rise to stiff guidewire simulation. When the shearing parameter is zero, the guidewire will be completely rigid and can not fall down under the influence of gravity. And Fig. 6(b) shows more complex guidewire deformation results obtained by respectively manipulating its soft tip with pulling, pushing, and twisting operations.

IV. Interactions with the Surrounding Environment

A. Model Coupling based on Virtual Links

To couple with the behaviors among guidewire, blood, and vessels, we uniformly construct volumetric chain-mails for vessel and blood flow field. Similar to the guidewire model, for each volumetric chain-mail, we connect it to its neighbors by real links, and set the compressing, stretching, and shearing constraints according to their heterogeneous properties respectively. As shown in Fig. 7, each vascular chain-mail is connected to its one-ring neighbors. For each chain-mail in the blood flow field, its neighboring chain-mails are determined by a sphere with certain radius.

In our PCI surgery simulator, the vessels deform with heart beating. The blood flow field, which is represented by millions of cells, should flow under the influence of vascular model via virtual links. Therefore, we should dynamically construct virtual vessel-blood links, because both of vessel and blood are moving. We respectively set the compressing, stretching, and shearing parameters for the virtual vessel-blood links to (1.0, 1.0, 0.0) to achieve close coupling. Suppose the sponsoring vascular chain-mail $\mathbf{p}$ moves to new position $\mathbf{p}^*$, based on the virtual link, the corresponding blood chain-mail $\mathbf{q}$ should move to new position $\mathbf{q}^*$ as

$$\mathbf{q}^* = \mathbf{q} + (\mathbf{p}^* - \mathbf{p}). \tag{11}$$

When the guidewire moves in the vessel, blood flow should affect the guidewire motion. Analogously, we also set the compressing, stretching, and shearing parameters for the virtual guidewire-blood links to (1.0, 1.0, 0.0). Suppose the current position of the guidewire chain-mail is $\mathbf{q}(x, y, z)$, one of its neighboring virtually-linked blood chain-mail is $\mathbf{p}_i(x, y, z, \mathbf{v})$, and $\mathbf{v}$ is the velocity. The guidewire motion induced by the virtual links can be calculated as

$$\left\{ \begin{array}{l} \mathbf{q}^* = \mathbf{q} + \sum_{i \in S} w_i \cdot \Delta\mathbf{p}_i \\ w_i = \frac{d_i}{\sum_{i \in S} d_i} \\ \Delta\mathbf{p}_i = \mathbf{v}_i \cdot \Delta t \end{array} \right. , \tag{12}$$

where S is the neighboring blood chain-mail set, w_i is the weight that is inversely proportional to the distance d_i

between guidewire chain-mail and its neighbors, and Δt is the time step.

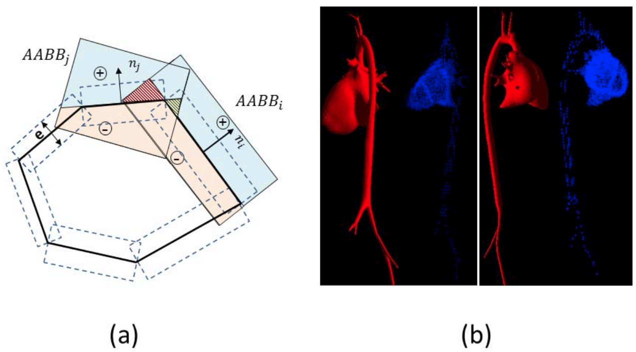

Figure 8. Illustration of collision handling. The Black polygon in (a) represents the vessel, $\vec{n}$ means the surface normal, dotted boxes are prisms of vascular mesh and solid-line boxes are AABB of dotted boxes, wherein different colors mean different SDF sign. (b) shows the heart and its SDF.

B. Collision Handling

We employ the sign distance field (SDF) method [23] to conduct collision detection. The distance field function of surface S together with its sign function are respectively defined as

$$D(p) = min\{|\mathbf{p} - \mathbf{q}|\}, \forall \mathbf{p} \in R^3, \mathbf{q} \in S \ , \tag{13}$$

$$sgn(p) = \begin{cases} -1, & if \ \langle \mathbf{p} - \mathbf{q} | \mathbf{n} \rangle < 0 \\ 1, & if \ \langle \mathbf{p} - \mathbf{q} | \mathbf{n} \rangle \geq 0 \end{cases} . \tag{14}$$

Here $\langle \cdot | \cdot \rangle$ denotes the inner product, $\mathbf{q}$ is $\mathbf{p}$'s closest point in S, and $\mathbf{n}$ is the surface normal.

The calculation of SDF is shown in Fig. 8(a). By extending the vascular triangles along the face normals, we can get the prisms, and calculate the axis-aligned bounding boxes (AABBs) for the prisms. Then we can compute the signed distance for each point in the bounding box. As shown in Fig. 8(b), the blue region represents parts of the negative distance field of the heart. If collision happens, collision response attempts to modify the chain-mail $\mathbf{p}_b$ to the legal position, and then we update the guidewire with the sponsoring chain-mail $\mathbf{p}_b$. To reduce the searching time and simplify the algorithm, we implement the collision detection based on CUDA.

As for the handling of collision response, we also calculate the signed distance d for each guidewire chain-mail $\mathbf{p}$ via the trilinear interpolation of its 8 corner points of the corresponding grid cell, and get the normal $\vec{n}$ by normalizing the analytic gradient of the trilinear interpolation. If a guidewire chain-mail is detected to be closer to the vessel than the given threshold ε or the chain-mail is outside the vessel, we modify its position via

$$\mathbf{p}^* = \mathbf{p} + \|\varepsilon - d\| \cdot \vec{n}. \tag{15}$$

And $\Delta \mathbf{p} = \mathbf{p}^* - \mathbf{p}$, the displacements along the normal direction $\Delta \mathbf{p}_n$, and the displacements along the tangential direction $\Delta \mathbf{p}_t$ can be calculated as

$$\begin{array}{l} \Delta \mathbf{p}_n = \mathbf{n} \cdot (\Delta \mathbf{p} \cdot \mathbf{n}) \\ \Delta \mathbf{p}_t = \Delta \mathbf{p} - \Delta \mathbf{p}_n \end{array} , \tag{16}$$

where $\mathbf{n}$ denotes the normal of the closest surface to the chain-mail $\mathbf{p}$.

To respect the friction behavior, we use Coulomb's model for friction computation, which considers both static and kinetic frictions. We can formulate the friction force as

$$\mathbf{F}_{friction} = -C_f * \Delta \mathbf{p}_t, 0 \leq C_f \leq 1 \ . \tag{17}$$

Specifically, we set $\beta = -max(\frac{\|\Delta \mathbf{p}_t\| - C_f \|\Delta \mathbf{p}_n\|}{\|\Delta \mathbf{p}_t\|}, 0)$ as a factor to indicate tangential movement, wherein $\beta = 0$ represents no movement and $\beta = 1$ means no friction. Therefore, we can rewrite the friction force formula as

$$\mathbf{F}_{friction} = (\beta - 1) \Delta \mathbf{p}_t \ . \tag{18}$$

C. Coupling Results

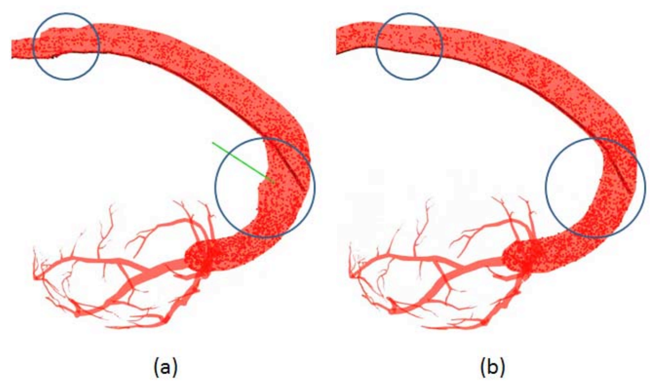

Figure 9. Demonstration of the guidewire-vessel coupling. When dragging a vessel chain-mail, under the influence of virtual links, the motions of the blood flow and guidewire are effected. The circles in (a) show the coupled deformation results, the corresponding circles in (b) show the deformation-reverted effects.

As shown in Fig. 9, through virtual links, we can easily achieve uniform cross-model coupling. When the influence of the blood flow is imposed, the guidewire tends to move along the direction of the blood flow. As shown in Fig. 10, the guidewire will stop until its tip collides with the vessel and the friction force between the guidewire and the vessel is large enough.

Besides, to verify the accuracy and stableness of our method, we respectively compare our inter-dynamic guidewire simulation result with those from position-based dynamics (PBD) method and Cosseart-based method. As

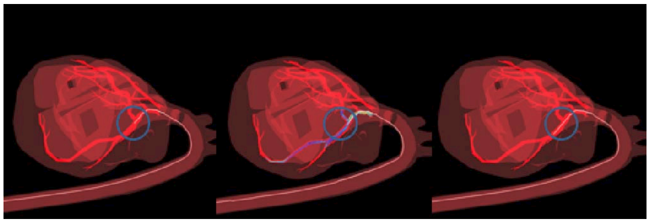

Figure 10. Demonstration of the guidewire-blood coupling. From left to right: the guidewire motion without flow field, blood flow field, and the guidewire motion with flow field. The color-encoded lines in the middle picture shows the flow velocities, wherein the colors indicates the speed while the direction of the line means the direction of the velocity.

shown in Fig. 11, for the complex heart and blood vessel models, our method is as stable as the well-recognized and popularly-used PBD method, and our method outperforms it in physical realism. Meanwhile, even though Cosseart-based method is completely based on physics and can achieve high fidelity, our method can also achieve comparable simulation results. However, Cosserat-based method is not only very unstable but also very inefficient when handling drastic force, frequent multi-point collision and long-time guidewire manipulation.

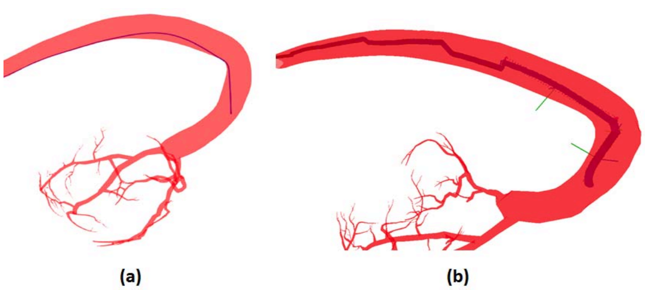

Figure 11. Comparison between our method and PBD method. (a) Our simulation result; (b) PBD simulation result.

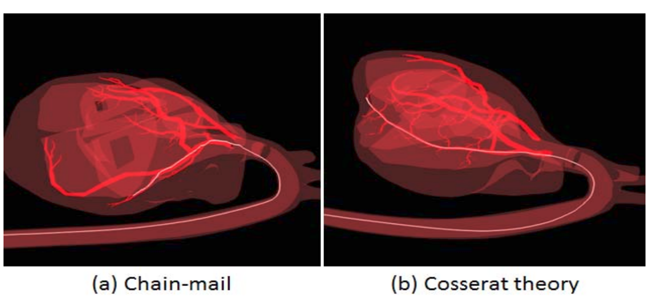

Figure 12. Comparison between our method and Cosseart-based method. (a) Our simulation result; (b) Cosseart-based simulation result.

V. Application In Virtual PCI Surgery

We integrate our guidewire simualtion into a PCI surgery simulator. Our PCI surgery simulator consists of six modules: (1) guidewire simulation, (2) blood flow simulation, (3) penalty force based haptic feedback calculation, (4) PCI-specific haptic instrument, (5) ray-casting based X-ray simulation, and (6) realistic rendering system. Guidewire is one of the most important instruments. Fig. 13 shows the workflow of our surgical simulator. The trainee controls the virtual instrument through the haptic device. And the haptic device is applied to connect the real guidewire to the virtual guidewire. When the trainee inserts the guidewire from aortic arch, and feeds it to the target location along the vessel via pushing and rotating operations, the force feedback is transmitted to the trainee by the haptic device at the same time, wherein the force feedback is calculated by summing the internal force and friction force resulted from the virtual guidewire as

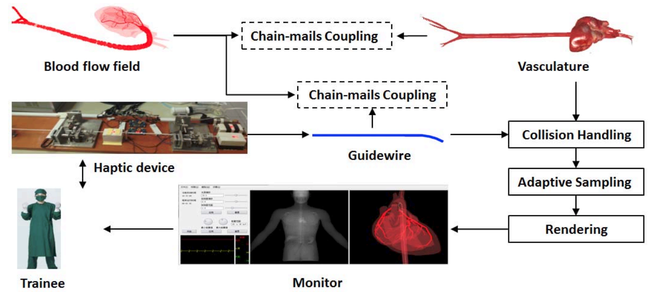

Figure 13. The workflow of guidewire manipulation and simulation in PCI simulator.

$$F_{feedback} = F_{friction} + F_{internal} \quad . \tag{19}$$

When the guidewire deform, the internal force can be calculated according to the displacement of the first two chain-mails with respects to its previous position. According to Hooke's law, we have

$$F_{internal} = (Length(P_1^t - P_2^t) - Length(P_1^{t-1} - P_2^{t-1})) \cdot k \quad , \tag{20}$$

where P_1^t and P_2^t are the current positions of the first two chain-mails, P_1^{t-1} and P_2^{t-1} are their previous positions, and k is the constant coefficient.

The guidewire simulation result in our PCI simulator is shown in Fig. 14. Our method can achieve physically-plausible guidewire simulation enabling inter-dynamics and heterogeneous interaction with the surrounding environment with unconditional-stableness and real-time efficiency, which can fully satisfy the actual requirements of PCI surgery simulation.

VI. Conclusion And Future Work

We have detailed a novel guidewire simulation method enabling inter-dynamics of the guidewire geometry, physical deformation, and their coupling with vessel wall and blood flow. Our new approach is based on the streamline of modeling, behavior, and interaction using the generalized,

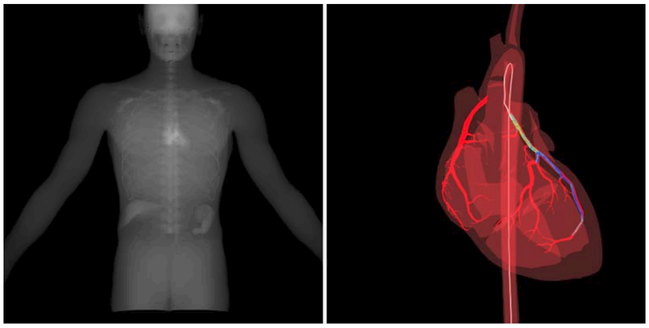

Figure 14. Demonstration of the guidewire simulation results in our PCI simulator.

heterogeneous chain-mails. As a result, our method allows the guidwire to freely move (forward or backward), bend, or twist subject to the surrounding flowing blood and beating vessel constraints as well as collision contact. Meanwhile, we have integrated our guidewire simulation into a prototype PCI surgery simulator equipped with haptic feedback. The observed stableness, real-time efficiency, flexibility, and high-fidelity realism collectively validate the effectiveness of our method and show great promise for its practical applications in clinical training fields.

However, currently we only consider the one-way coupling that comes from vessel and blood to guidewire, but ignore the guidewire' influence on the motion of blood and vessel. We plan to continue to improve our system's performance via two-way coupling in order to make our PCI simulator more realistic and practical for medical practitioners.

Acknowledgments. This research is supported in part by National Natural Science Foundation of China (No. 61190120, 61190121, 61190125, and 61300067) and National Science Foundation of USA (No. IIS-0949467, IIS-1047715, and IIS-1049448).

REFERENCES

[1] S. Schafer, V. Singh, P. B. Noël, A. M. Walczak, J. Xu, and K. R. Hoffmann, "Real-time endovascular guidewire position simulation using shortest path algorithms," *International journal of computer assisted radiology and surgery.*, vol. 4, no. 6, pp. 597–608, 2009.

[2] M. Luo, H. Xie, L. Xie, P. Cai, and L. Gu, "A robust and real-time vascular intervention simulation based on kirchhoff elastic rod," *Computerized Medical Imaging and Graphics.*, vol. 38, no. 8, pp. 735–743, 2014.

[3] Y. Mao, F. Hou, S. Li, A. Hao, M. Ai, and H. Qin, "Robust and high-fidelity guidewire simulation with applications in percutaneous coronary intervention system," in *Proceedings of the 19th ACM Symposium on Virtual Reality Software and Technology*. ACM, 2013, pp. 27–30.

[4] J. Bender, M. Müller, M. A. Otaduy, and M. Teschner, "Position-based methods for the simulation of solid objects in computer graphics," *EUROGRAPHICS 2013 State of the Art Reports*, 2013.

[5] T. Liu, A. W. Bargteil, J. F. O'Brien, and L. Kavan, "Fast simulation of mass-spring systems," *ACM Transactions on Graphics (TOG).*, vol. 32, no. 6, p. 214, 2013.

[6] V. Luboz, J. Zhai, P. Littler, T. Odetoyinbo, D. Gould, T. How, and F. Bello, "Endovascular guidewire flexibility simulation," in *Biomedical Simulation*. Springer, 2010, pp. 171–180.

[7] V. Luboz, R. Blazewski, D. Gould, and F. Bello, "Real-time guidewire simulation in complex vascular models," *The Visual Computer.*, vol. 25, no. 9, pp. 827–834, 2009.

[8] S.-H. Mi, Z.-G. Hou, F. Yang, X.-L. Xie, and G.-B. Bian, "A multi-body mass-spring model for virtual reality training simulators based on a robotic guide wire operating system," in *Robotics and Biomimetics (ROBIO), 2013 IEEE International Conference on*. IEEE, 2013, pp. 2031–2036.

[9] P. Wei, Z.-Q. Feng, X.-L. Xie, G.-B. Bian, and Z.-G. Hou, "Fem-based guide wire simulation and interaction for a minimally invasive vascular surgery training system," in *Intelligent Control and Automation (WCICA), 2014 11th World Congress on*. IEEE, 2014, pp. 964–969.

[10] S. Li, J. Guo, Q. Wang, Q. Meng, Y.-P. Chui, J. Qin, and P.-A. Heng, "A catheterization-training simulator based on a fast multigrid solver," *Computer Graphics and Applications, IEEE.*, vol. 32, no. 6, pp. 56–70, 2012.

[11] W. Tang, P. Lagadec, D. Gould, T. Wan, J. Zhai, and T. How, "A realistic elastic rod model for real-time simulation of minimally invasive vascular interventions," *The Visual Computer*, vol. 26, no. 9, pp. 1157–1165, 2010.

[12] S. Sueda, G. L. Jones, D. I. W. Levin, and D. K. Pai, "Large-scale dynamic simulation of highly constrained strands," in *ACM SIGGRAPH 2011 papers*, ser. SIGGRAPH '11, 2011, pp. 39:1–39:10.

[13] J. M. Kaldor, D. L. James, and S. Marschner, "Simulating knitted cloth at the yarn level," *ACM Trans. Graph.*, vol. 27, no. 3, pp. 65:1–65:9, Aug. 2008.

[14] A. Theetten, L. Grisoni, C. Andriot, and B. Barsky, "Geometrically exact dynamic splines," *Computer-Aided Design.*, vol. 40, no. 1, pp. 35–48, 2008.

[15] Y. Ganji and F. Janabi-Sharifi, "Catheter kinematics for intracardiac navigation," *IEEE Transactions on Biomedical Engineering.*, vol. 56, no. 3, pp. 621–632, Mar. 2009.

[16] W. Rungjiratananon, Y. Kanamori, and T. Nishita, "Chain shape matching for simulating complex hairstyles," *Computer Graphics Forum.*, vol. 29, no. 8, pp. 2438–2446, 2010.

[17] N. Akinci, M. Ihmsen, G. Akinci, B. Solenthaler, and M. Teschner, "Versatile rigid-fluid coupling for incompressible sph," *ACM Transactions on Graphics (TOG).*, vol. 31, no. 4, p. 62, 2012.

[18] W.-C. Lin, "Coupling hair with smoothed particle hydrodynamics fluids," 2014.

[19] M. Servin, C. Lacoursiére, F. Nordfelth, and K. Bodin, "Hybrid, multiresolution wires with massless frictional contacts," *IEEE Transactions on Visualization and Computer Graphics.*, vol. 17, no. 7, pp. 970–982, jul. 2011.

[20] D. Durville, "Contact-friction modeling within elastic beam assemblies: an application to knot tightening," *Computational Mechanics.*, vol. 49, no. 6, pp. 687–707, 2012.

[21] S. F. Gibson, "3d chainmail: a fast algorithm for deforming volumetric objects," in *Proceedings of the 1997 symposium on Interactive 3D graphics*. ACM, 1997, pp. 149–ff.

[22] Y. Li and K. Brodlie, "Soft object modelling with generalised chainmailłextending the boundaries of web-based graphics," in *Computer Graphics Forum*, vol. 22, no. 4. Wiley Online Library, 2003, pp. 717–727.

[23] A. Fuhrmann, G. Sobotka, and C. Groß, "Distance fields for rapid collision detection in physically based modeling," in *Proceedings of GraphiCon 2003*, 2003, pp. 58–65.